Feature Extraction in Pet Images for the Diagnosis of Alzheimer's Disease

João Duarte, Helena Aidos and Ana Fred
Instituto de Telecomunicações, Instituto Superior Técnico, Lisbon, Portugal

Keywords: Computer-Aided Diagnosis, Image Classification, Image segmentation, Alzheimer's Disease.

Abstract: Alzheimer's disease accounts for an estimated 60% to 80% of cases of dementia and its victims are mainly elderly people. Recently, several computer-aided diagnosis systems have been developed, based on extracting information from FDG-PET scans. 3-dimensional FDG-PET images, under a voxel-as-feature approach, lead to high-dimensional feature spaces, which results in system performance problems. In order to reduce the dimensionality of these images, multi-scale methods may be used as feature extraction. We propose a multi-scale approach for feature extraction of 3-dimensional images to improve the performance of a diagnosis system using clustering techniques. To evaluate the performance of our approach we applied it to a database obtained from Alzheimer's Disease Neuroimaging Initiative (ADNI) and compare it with Gaussian pyramid technique. Experimental results have shown that the proposed approach is a good option for image feature reduction, outperforming the Gaussian pyramid technique.

1 INTRODUCTION

Alzheimer's disease (AD) is the most common type of dementia and is characterized by gradual increasing difficulty in remembering new information, caused by disruption of brain cell function, which usually starts in brain regions responsible for forming new memories (Alzheimer's Association, 2013). Mild cognitive impairment (MCI) is a condition in which a patient has noticeable decreased thinking abilities, but does not restrain the individual to perform everyday activities (Alzheimer's Association, 2013). People with MCI have higher probabilities of developing AD than cognitive normal (CN) people.

The early diagnosis of AD is very important to allow the patients, and their families, to take the necessary arrangements that empowers patients to live independently as long as possible, and find alternatives when this is not possible. Despite AD has no cure, early diagnosis may improve life quality and extend life expectancy by enabling treatments to delay the progression of AD symptoms. In order to facilitate early diagnosis of the AD/MCI conditions, several computer-aided diagnosis (CAD) systems have been proposed, usually relying in processing of neuroimages, such as, fluorodeoxyglucose positron emission tomography (FDG-PET) (Gray et al., 2012; Martínez-Murcia et al., 2012; Illán et al., 2011), magnetic resonance imaging (MRI) (Natarajan et al., 2012; Maldjian et al., 2003), and single photon emission computed tomography (SPECT) images (Ramirez et al., 2013). Also, some CAD systems combine several of the previous imaging modalities (Gray et al., 2013; Dukart et al., 2011; Zhang et al., 2011)

Analysis of neuroimages typically translates in high-dimensional feature spaces, leading to system performance problems (i.e. high computational and memory costs), and also tends to lower the accuracy of the diagnosis. Hence, different techniques should be used to reduce the dimensionality of the neuroimages. Various feature extraction techniques have been applied for the diagnosis of Alzheimer's disease (Segovia et al., 2012; Morgado et al., 2013b), which are very important as the resulting features are used to differentiate between AD, MCI and CN conditions. Also, several feature selection techniques (Savio and Graña, 2013; Morgado, 2012) have been used to identify which (and how many) of these features should be used by the classification algorithms, since many of the features are redundant or may not have discriminative power. The selected features may be thought as a partial view of the brain containing the most relevant regions of it, and some studies have shown that using them improves accuracy (Morgado et al., 2013a). Other studies suggest that using volumes-of-interest may be worse that using whole-brain information when a single imaging modality is used, although when using several imaging modalities

Duarte J., Aidos H. and Fred A..
Feature Extraction in Pet Images for the Diagnosis of Alzheimer's Disease.
DOI: 10.5220/0004808705610568
In *Proceedings of the 3rd International Conference on Pattern Recognition Applications and Methods* (ICPRAM-2014), pages 561-568
ISBN: 978-989-758-018-5

the converse may be preferable (Dukart et al., 2011; Dukart et al., 2013).

We present a dimensionality reduction approach based on data clustering to reduce the high-dimensional feature space of neuroimages. This approach may be used with several imaging modalities and/or combined with other feature extraction techniques. In this paper, our approach is applied to the voxel intensities of FDG-PET images and compared with a scale-space representation using the Gaussian pyramid technique in three classification problems: AD vs CN, MCI vs CN, and AD vs MCI.

The remaining of this paper is organized as follows. Section 2 describes the feature extraction, selection, and classification steps included in the methodology presented in this paper. Section 3 exhibits the data set, the experimental design and the corresponding results. Finally, section 4 concludes this paper.

2 METHODOLOGY

Our goal is to diagnose the condition of a given patient using its FDG-PET scan by learning from a set of labeled images whose conditions are known. We use voxel intensities, $V(x,y,z)$, obtained directly from the FDG-PET scan, to identify the condition of a patient. $V(x,y,z)$ denotes the value of the FDG uptake detected at the voxel located at the space position (x,y,z), where x, y and z are integer numbers.

Our methodology to build a computer-aided diagnosis system capable of distinguishing different patient conditions has three steps: reduce the number of features to improve system performance; select the most important features; and, finally, train a classification algorithm. Note that, in this work we focus in comparing feature extraction methods, namely, one using the Gaussian pyramid and another using data clustering. We also compare the previous techniques that reduce the number of features with one strategy that uses the whole-brain information. Also, we are using the voxel intensities of FDG-PET images but other imaging modalities, such as MRI or SPECT, could be used instead.

2.1 Feature Extraction using the Gaussian Pyramid

A problem when dealing with a 3-dimensional FDG-PET image is the huge amount of features it contains, which may degrade the performance of pattern recognition algorithms. However, the intensities of voxels that are close in space tend to be similar and, consequently, some redundant information may be eliminated.

The Gaussian pyramid (Burt, 1981) is a technique that creates a sequence of images which are smoothed using a Gaussian average, and then scaled down. These images are successively smaller due to subsampling, and each voxel at a given level contains the average neighborhood's voxel intensity of the corresponding voxel on the previous level of the pyramid.

The technique works as follows. In the first step, the image is smoothed as

$$V_l(x,y,z) = \sum_{m=-2}^{2}\sum_{n=-2}^{2}\sum_{o=-2}^{2} w(m,n,o)V_{l-1}(2x+m,2y+n,2z+o), \quad (1)$$

for $l = 1,2,\cdots$, with $V_0(x,y,z) = V(x,y,z)$ where V_l represents the l^{th} level of the pyramid, and $w(m,n,o) = w(m)\cdot w(n)\cdot w(o)$ is a weighting function or generating kernel. The level 0 corresponds to the original image. The generating kernel used in this work has width 5 and is defined as $w(m) = w(n) = w(o) = \mathbf{w}_{m+3}$, $m \in \{-2,-1,\cdots,2\}$, where $\mathbf{w} = \frac{1}{16}[1\,4\,6\,4\,1]$, which resembles a Gaussian function. In the second step, the image is subsampled by a factor of two in each of the dimensions.

Figure 1 shows an example of applying the Gaussian pyramid to a $128\times128\times60$ FDG-PET image (a slice for each image is shown).

2.2 Feature Extraction using Data Clustering

We propose to perform feature extraction using a data clustering algorithm. The objective of data clustering consists of dividing a data set, $\mathcal{X}$, composed of n data objects $\{x_1,\cdots,x_n\}$, into K clusters $\{C_1,\cdots,C_K\}$ such that similar objects, x_i, x_j, are placed in the same cluster, i.e $\{x_i,x_j\} \in C_k$, and dissimilar objects are grouped in different clusters, i.e. $x_i \in C_k, x_j \in C_l, k \neq l$. The resulting labels of a partition $P = \{P_1,\cdots,P_n\}$ indicate the cluster to which each object belongs. We intend to group voxels in a FDG-PET image into clusters to reduce redundant information and, consequently, decrease the number of features for the classification task. The clusters should represent regions in the 3-dimensional space with similar voxel intensities. The methodology to find these regions is explained in the following.

Let $V^p(x,y,z)$ represent the voxel (x,y,z) of the p^{th} FDG-PET image in a database containing q images. First, a *mean brain image* V^* is computed by averaging the corresponding voxel (x,y,z) over the entire population:

$$V^*(x,y,z) = \frac{1}{q}\sum_{i=1}^{q} V^i(x,y,z). \quad (2)$$

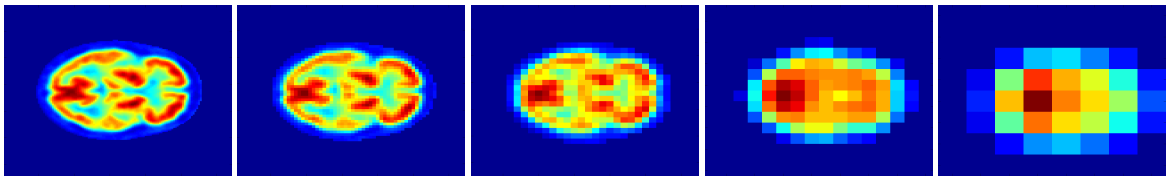

(a) Original (b) Level 1 (c) Level 2 (d) Level 3 (e) Level 4

Figure 1: Gaussian pyramid example from a slice of a 3-dimensional FDG-PET image (all images are zoomed to the same size).

Then, the voxels corresponding to background are discarded, and the remaining n voxel intensities, $V^*(x,y,z)$, are stacked into a vector $f = [f_1, \cdots, f_n]^T$.

A vectorial representation of the data set $\mathbf{X} \in \mathbb{R}^{n\times 4}$ is built considering both the voxel intensities and the corresponding position in space. This representation is defined as

$$\mathbf{X} = \begin{bmatrix} f_1 & posX(1) & posY(1) & posZ(1) \\ f_2 & posX(2) & posY(2) & posZ(2) \\ \vdots & \vdots & \vdots & \vdots \\ f_n & posX(n) & posY(n) & posZ(n) \end{bmatrix}, \quad (3)$$

where $posX(i)$, $posY(i)$, $posZ(i)$ are functions that indicate the space position of the i^{th} voxel in each axis of the 3-dimensional space. In order to bring all of the dimensions into proportion with one another, a normalization step is performed such that: a) all dimensions have mean 0; b) the 3 dimensions corresponding to space location have standard deviation 1; c) and the dimension corresponding to the voxel intensity have standard deviation $\alpha > 0$. α is a parameter that influences the importance of voxel intensity in clustering.

Next, a partition of $\mathbf{X}$ into K clusters is obtained by applying a clustering algorithm to it, and the labels P_i, $\forall i \in \{1, \cdots, n\}$, are used to identify the regions in space.

Finally, a new representation for each image V^i is build containing K features (one for each cluster). The value for each feature k for a patient i is computed as the average intensity of the voxels belonging to the corresponding cluster C_k. Figure 2 shows an example of this approach. Images obtained using a high number of clusters are very similar to the original one, while images obtained using few clusters are smother.

The proposed approach has two main advantages over the Gaussian pyramid approach: it is very easy to specify the number of features by simply specifying the number of clusters to the clustering algorithm; and each resulting feature may represent space regions with distinct shapes and size, thus the features are more meaningful.

The well-known K-means algorithm (MacQueen, 1967) was chosen to perform the brain segmentation, due to its low-computational cost, using random initialization of the centroids, however any clustering algorithm could be used instead. K-means (locally) minimizes the within-cluster sum of squares: $\sum_{k=1}^{K} \sum_{\mathbf{x}_i \in C_k} ||\mathbf{x}_i - \bar{\mathbf{x}}_k||^2$, where $||\mathbf{x}_i - \bar{\mathbf{x}}_k||^2$ is the Euclidean distance between $\mathbf{x}_i$ and its closest cluster centroid $\bar{\mathbf{x}}_k$.

2.3 Feature Selection using Mutual Information

Feature selection is the process of choosing a subset of features in a data set. The resulting data representation should improve the performance of classifiers, reduce computational and memory costs, and facilitate data visualization and data understanding (Guyon and Elisseeff, 2003). To reduce the number of features for our task, we use mutual information (MI) between features and class labels to rank the features and choose the ones with higher value. Let $\mathbf{F} \in \mathbb{R}^n$ be a vector representing a feature in a data set, f_i, $i \in \{1, \cdots, n\}$ its value for the i^{th} individual in a population of size n, and F a random variable representing the distribution of $\mathbf{F}$ obtained by building a histogram with m bins. Also, let Y be a random variable representing the labels of the population containing c classes. The mutual information between the feature F and the labels Y is computed as

$$MI = \sum_{j=1}^{m} \sum_{i=1}^{c} P(F=j, Y=i) \log \frac{P(F=j, Y=i)}{P(F=j)P(Y=i)}, \quad (4)$$

where $P(F=j)$ is the probability of the j^{th} bin, and $P(Y=i)$ the probability if the i^{th} class.

2.4 Image Classification

Once the feature extraction and the feature selection steps are conducted, a supervised classification algorithm is applied as the final step of the diagnostic problem. In the learning phase, a classification algorithm produces a function, using labeled data, capable of assigning appropriate labels to unlabeled examples. In this case, given non-redundant and labeled representations of FDG-PET scans, the algorithm learns to identify the condition of a new FDG-PET image. In

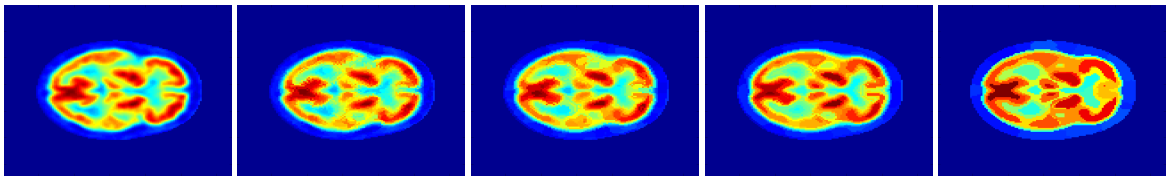

(a) Original (b) K=36209 (c) K=4723 (d) K=656 (e) K=111

Figure 2: Example of applying the clustering methodology to a $128 \times 128 \times 60$ FDG-PET image (only a slice for each image is shown).

Table 1: Clinical and demographic characteristics of each class. Age and MMSE (Mini Mental State Exam) are represented by the corresponding mean values and standard deviations.

Attributes	AD	MCI	CN
Number of subjects	59	59	59
Age	78.26 (±6.62)	77.71 (±6.88)	77.38 (±4.87)
Sex (% of males)	57.63	67.80	64.41
MMSE	19.60 (±5.06)	25.68 (±2.97)	29.20 (±0.92)

this paper, we consider three classification tasks: AD vs CN, MCI vs CN, and AD vs MCI.

3 EXPERIMENTS

3.1 Data Set

In this study, we used FDG-PET images for AD, MCI and CN subjects, retrieved from the ADNI database. The subjects were chosen to obey a certain criteria: the Clinical Dementia Rating (CDR) should be 0.5 or higher for AD patients, 0.5 for MCI patients and 0 for CN. This selection results in a dataset composed by 59, 142 and 84 subjects for AD, MCI and CN, respectively. Since our task is classification using the SVM algorithm, we decided to balanced the classes. In that sense, 59 subjects from each MCI and CN groups were selected randomly. Table 1 summarizes some clinical and demographic information.

The FDG-PET images have been pre-processed to minimize differences between images: each image was co-registered, averaged, reoriented (the anterior-posterior axis of each subject was parallel to the AC-PC line), normalized in its intensity, and smoothed to uniform standardized resolution. Details of the pre-processing are available in the ADNI project web-page[1].

[1] http://adni.loni.usc.edu/methods/pet-analysis/pre-processing/

3.2 Experimental Design

To assess the performance of the two feature extraction approaches, we applied the methodology described in section 2. We chose the Support Vector Machine (SVM) (Cortes and Vapnik, 1995) using a linear kernel as the classifier. The reason for this preference lies in the SVM being a common choice for the purpose.

We applied the Gaussian pyramid technique to the original voxel intensities to obtain 4 levels of feature extraction. The clustering approach was performed, also using the original voxel intensities, by applying the K-means algorithm, setting the number of clusters to the number of features obtained by the Gaussian pyramid technique, so that we can fairly compare both approaches. The values 2, 4 and 8 were tested for the α parameter. Also, after the feature extraction step, the feature selection step was tested using several number of features, as shown in table 2. After some empirical testing, the number of bins to build the features histograms for MI computation was set to 8, so that each bin could have a meaningful number of points.

The parameter which controls the cost of misclassification in the SVM was tuned from the set $C \in \{2^{-16}, 2^{-14}, 2^{-12}, 2^{-10}, 2^{-8}, 2^{-6}, 2^{-4}, 2^{-2}, 2^{0}, 2^{2}, 2^{4}\}$ using a 10×10 nested cross-validation procedure (Varma and Simon, 2006). The nested cross-validation procedure was repeated 20 times for better performance assessment.

3.3 Results

Figure 3 shows the mean accuracies obtained for the AD vs CN problem using the Gaussian pyramid with 4 levels, and the clustering approach with the corresponding number of clusters. Figure 3a depicts the results obtained for the level 1 of the Gaussian pyramid and for applying K-means with 36209 clusters. The clustering approach with $\alpha = 8$ obtained the best accuracy of 87.56% using 2500 features, followed by the Gaussian pyramid using 250 features with 87.55%. The differences are not significant in

Table 2: Number of features for each level of the Gaussian pyramid (background removed) and corresponding number of features tested for the feature selection step.

Level	Total number of features	Number of selected features
1	36209	50, 100, 250, 500, 1000, 2500, 5000, 10000, 25000, 36209
2	4723	50, 100, 250, 500, 1000, 2500, 4723
3	656	50, 100, 250, 500, 656
4	111	50, 100, 111

this case. Figure 3b shows the results for the second level of the Gaussian pyramid technique and for K-means with 4723 clusters. The clustering approach with $\alpha = 2$ achieved the best mean accuracy (88.14%) using 1000 features. In general, the clustering approach was better than the Gaussian pyramid, for all values of α. The results for the level 3 of Gaussian pyramid and the clustering approach with 656 clusters are presented in figure 3c. Usually, the clustering approach was better than the Gaussian pyramid for all values of α, being the best result of 88.21% obtained using K-means with α set to 4. Figure 3c presents the results for the fourth level of the Gaussian pyramid and the corresponding clustering approach with 111 clusters. Again, the clustering approach almost always outperforms the Gaussian pyramid for all values of α. The best result in this case was 84.94% using $\alpha = 2$. The overall best result for the AD vs CN problem was obtained by reducing the original number of features to 656 using the clustering approach with $\alpha = 4$, and then selecting the best 500 features to train the classifier.

Figure 4 presents the results for the MCI vs CN problem. The best results obtained for the level 1 of the Gaussian pyramid was 79.45%, and 79.5% for the corresponding number of clusters for K-means, as shown in figure 4a. Figure 4b presents the results for the second level of the pyramid and for the clustering approach with 4723 clusters. Generally, K-means with $\alpha = 2$ obtains good results, but the highest accuracy (78.88%) was achieved by setting $\alpha = 8$ and selecting the top 2500 features. For the level 3 and 4 of the Gaussian pyramid and the corresponding number of clusters for the clustering approach, it can be seen in figures 4c and 4d that the clustering approaches with $\alpha = 2$ and $\alpha = 4$ are clearly better than the Gaussian pyramid technique. Overall, the K-means with 656 clusters obtained, again, the highest mean accuracy (80.22%), selecting the top 250 features.

Figure 5 shows the results for the AD vs MCI problem. For the case of the level 1 of the Gaussian pyramid and the corresponding clustering results (figure 5a), it can be seen that all feature extraction methods perform better using a small number of features. The best result was achieved by K-means with 72.36% using the top 100 features and $\alpha = 2$. Figure

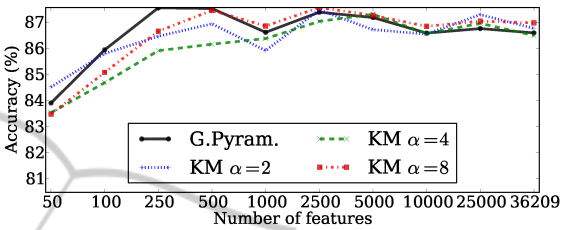

(a) Gaussian pyramid level 1, K-means 36209 clusters.

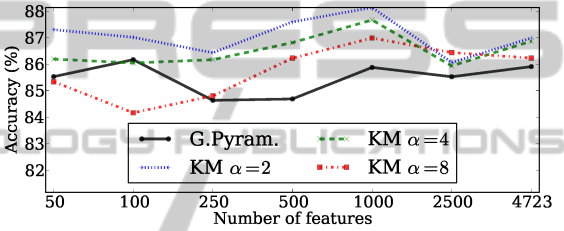

(b) Gaussian pyramid level 2, K-means 4723 clusters.

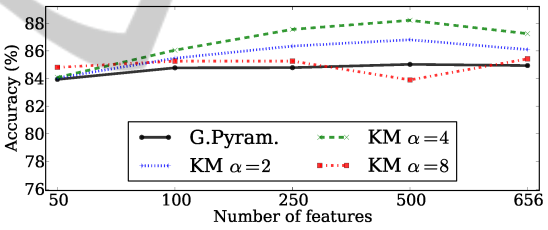

(c) Gaussian pyramid level 3, K-means 656 clusters.

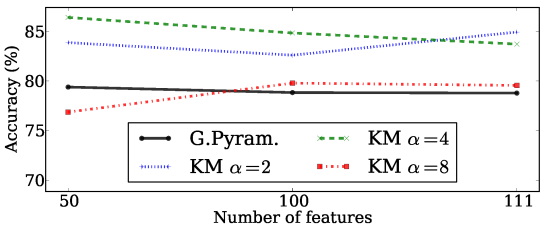

(d) Gaussian pyramid level 4, K-means 111 clusters.

Figure 3: Mean accuracies obtained for the AD vs CN problem using both the Gaussian pyramid and the data clustering approach.

5b shows the mean accuracies for the second level of the pyramid and for the clustering approach with 4723 clusters. As above, the best results were obtained using few features. K-means achieved again the best accuracy with 70.31% using only 50 features and with $\alpha = 8$. Figures 5c and 5d presents the results for the last two levels of the Gaussian pyramid and the cor-

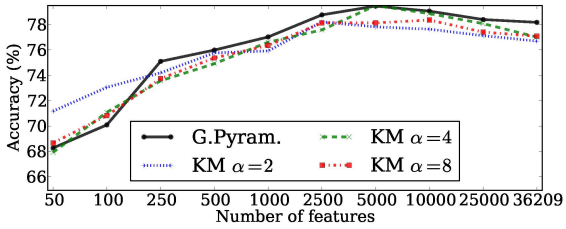

(a) Gaussian pyramid level 1, K-means 36209 clusters.

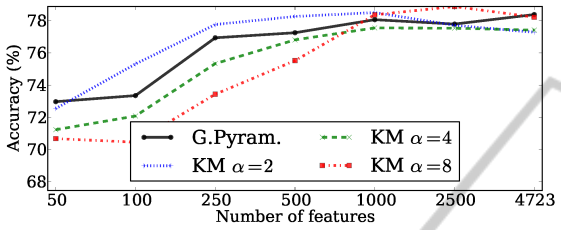

(b) Gaussian pyramid level 2, K-means 4723 clusters.

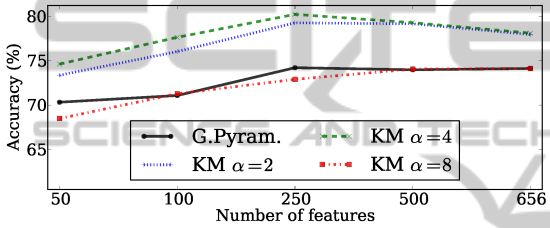

(c) Gaussian pyramid level 3, K-means 656 clusters.

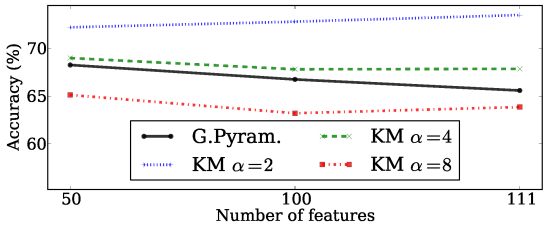

(d) Gaussian pyramid level 4, K-means 111 clusters.

Figure 4: Mean accuracies obtained for the MCI vs CN problem using both the Gaussian pyramid and the data clustering approach.

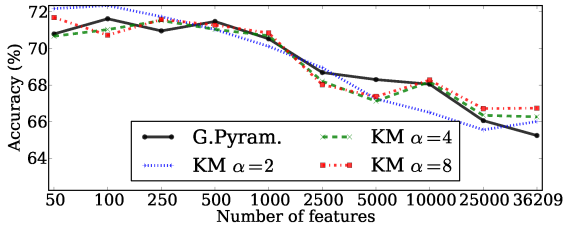

(a) Gaussian pyramid level 1, K-means 36209 clusters.

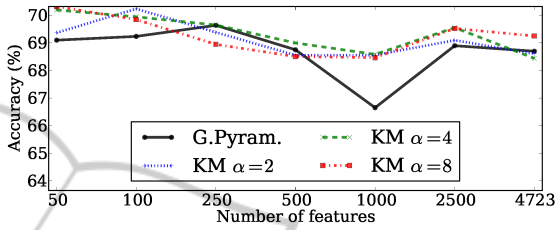

(b) Gaussian pyramid level 2, K-means 4723 clusters.

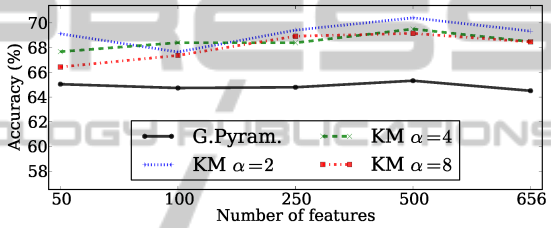

(c) Gaussian pyramid level 3, K-means 656 clusters.

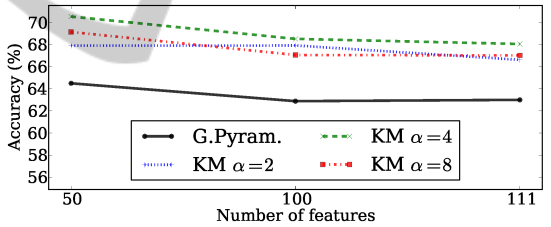

(d) Gaussian pyramid level 4, K-means 111 clusters.

Figure 5: Mean accuracies obtained for the AD vs MCI problem using both the Gaussian pyramid and the data clustering approach.

responding clustering results. It can be clearly seen that the clustering approach outperforms the Gaussian pyramid technique for all values of α. In the first case, the best result is obtained by K-means using 500 features and $\alpha = 2$ with 70.42%, which is significantly higher than the 65.33% achieved by the Gaussian pyramid. For the second case, the best result of 70.55% was achieved by setting $\alpha = 4$ and selecting the top 50 features, which is much superior that the 64.50% obtained by the Gaussian pyramid technique. Overall, the best accuracy for the AD vs MCI problem (72.34%) was obtained by clustering the original features with 36209 clusters with $\alpha = 2$ and selecting the top 100 features.

Next, we will compare the previous results with the methodology without feature extraction, i.e., applying feature selection directly over the original voxel intensities. Figure 6 presents the corresponding mean accuracies. This representation contains 297735 features, corresponding to the voxel intensities of the original images after removing the back-

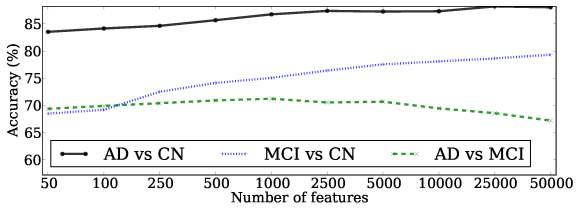

Figure 6: Mean accuracies obtained for the AD vs CN, MCI vs CN, and AD vs MCI using the original voxel intensities (i.e. without feature extraction).

Table 3: Best mean accuracy values and standard deviations obtained by not using any feature extraction technique and the corresponding results for the best approach using feature extraction.

		AD vs CN	MCI vs CN	AD vs MCI
Without Feature Extraction	**Accuracy**	88.22%	79.34%	71.25%
	Standard Deviation	1.19%	2.45%	1.70%
	#Selected Features	25000	50000	1000
With Feature Extraction	**Accuracy**	88.21%	80.22%	72.34%
	Standard Deviation	1.67%	2.27%	1.66%
	Feat. Sel. Approach	K-means $\alpha = 4$	K-means $\alpha = 4$	K-means $\alpha = 2$
	#Reduced Features	656	656	36209
	#Selected Features	500	250	100

ground. For the AD vs CN and MCI vs CN problems, the accuracy increases as the number of selected features grows. The best results were 88.22% for the AD vs CN classification task and 79.34% for the MCI vs CN problem. For the AD vs MCI classification task, high number of features leads to lower accuracies. The best result in this case was 71.25%. A summary showing the best results achieved with and without performing feature extraction is presented in table 3. The main conclusion is that using the proposed clustering approach have similar results in the AD vs CN, and better results in the MCI vs CN and AD vs MCI using far fewer features.

4 CONCLUSIONS AND FUTURE WORK

A new approach to reduce features in neuroimages was proposed based on clustering similar brain regions with respect to both voxel intensity values and voxel space positions. We integrated it in a methodology for performing computer-aided diagnosis of Alzheimer's disease and mild cognitive impairment conditions, and compared it with the Gaussian pyramid technique.

Results have shown that the proposed approach outperforms the Gaussian pyramid technique for feature reduction. This is more evident when the brain is represented by a lower number of features, suggesting that the clustering approach is more robust. Also, the proposed feature extraction technique leads to similar or better classification accuracies than using the original voxel intensities but using a small fraction of the number of features, which allows the development of computer-aided diagnosis systems with fewer processing and memory requirements.

In future work we intend to use constrained clustering algorithms, capable of using *a priori* information about specific domains. Our idea is to map information about the neighborhood of the voxels as constraints in order to improve the brain segmentation. We will also compare these approaches with recent multi-scale techniques.

ACKNOWLEDGEMENTS

This work was supported by the Portuguese Foundation for Science and Technology grants PTDC/SAU-ENB/114606/2009 and PTDC/EEI-SII/2312/2012.

REFERENCES

Alzheimer's Association (2013). Alzheimer's disease facts and figures Alzheimer's association. *ALZHEIMERS & DEMENTIA*, 9(2):208–245.

Burt, P. J. (1981). Fast filter transform for image processing. *Comp. graphics and image proc.*

Cortes, C. and Vapnik, V. (1995). Support-vector networks. *Mach. Learn.*, 20(3):273–297.

Dukart, J., Mueller, K., Barthel, H., Villringer, A., Sabri, O., and Schroeter, M. L. (2013). Meta-analysis based SVM classification enables accurate detection of Alzheimer's disease across different clinical centers using FDG-PET and MRI. *Psych. Res.: Neuroimaging*, 212(3):230 – 236.

Dukart, J., Mueller, K., Horstmann, A., Barthel, H., Möller, H. E., Villringer, A., Sabri, O., and Schroeter, M. L. (2011). Combined evaluation of FDG-PET and MRI improves detection and differentiation of dementia. *PLoS ONE*, 6(3).

Gray, K., Wolz, R., Heckemann, R., Aljabar, P., Hammers, A., and Rueckert, D. (2012). Multi-region analysis of longitudinal FDG-PET for the classification of Alzheimer's disease. *NeuroImage*, 60(1):221–229.

Gray, K. R., Aljabar, P., Heckemann, R. A., Hammers, A., and Rueckert, D. (2013). Random forest-based similarity measures for multi-modal classification of Alzheimer's disease. *NeuroImage*, 65(0):167 – 175.

Guyon, I. and Elisseeff, A. (2003). An introduction to variable and feature selection. *J. Mach. Learn. Res.*, 3:1157–1182.

Illán, I. A., Górriz, J. M., Ramírez, J., Salas-Gonzalez, D., López, M. M., Segovia, F., Chaves, R., Gómez-Rio, M., and Puntonet, C. G. (2011). ^{18}F-FDG PET imaging analysis for computer aided Alzheimer's diagnosis. *Inf. Sci.*, 181(4):903–916.

MacQueen, J. B. (1967). Some methods for classification and analysis of multivariate observations. In Cam, L. M. L. and Neyman, J., editors, *Proc. of the fifth Berkeley Symposium on Mathematical Statistics and Probability*, volume 1, pages 281–297. University of California Press.

Maldjian, J. A., Laurienti, P. J., Kraft, R. A., and Burdette, J. H. (2003). An automated method for neuroanatomic and cytoarchitectonic atlas-based interrogation of fMRI data sets. *NeuroImage*, 19(3):1233 – 1239.

Martínez-Murcia, F. J., Górriz, J. M., Ramírez, J., Puntonet, C. G., and Salas-Gonzalez, D. (2012). Computer aided diagnosis tool for Alzheimer's disease based on Mann-Whitney-Wilcoxon u-test. *Expert Syst. Appl.*, 39(10):9676–9685.

Morgado, P., Silveira, M., and Marques, J. (2013a). Efficient selection of non-redundant features for the diagnosis of Alzheimer's disease. In *Biomedical Imaging (ISBI), 2013 IEEE 10th International Symposium on*, pages 640–643.

Morgado, P., Silveira, M., and Marques, J. S. (2013b). Diagnosis of Alzheimer's disease using 3D local binary patterns. *Computer Methods in Biomechanics and Biomedical Engineering: Imaging & Visualization*, 1(1):2–12.

Morgado, P. M. M. (2012). Automated diagnosis of Alzheimer's disease using PET images. Master's thesis, Instituto Superior Técnico - Universidade Técnica de Lisboa.

Natarajan, S., Joshi, S., Saha, B. N., Edwards, A., Khot, T., Moody, E., Kersting, K., Whitlow, C. T., and Maldjian, J. A. (2012). A machine learning pipeline for three-way classification of Alzheimer patients from structural magnetic resonance images of the brain. In *ICMLA*, pages 203–208.

Ramirez, J., Gorriz, J., Salas-Gonzalez, D., Romero, A., Lopez, M., Alvarez, I., and Gomez-Rio, M. (2013). Computer-aided diagnosis of Alzheimer's type dementia combining support vector machines and discriminant set of features. *Information Sciences - Prediction, Control and Diagnosis using Advanced Neural Computations*, 237(0):59 – 72.

Savio, A. and Graña, M. (2013). Deformation based feature selection for computer aided diagnosis of Alzheimer's disease. *Expert Systems with Applications*, 40(5):1619 – 1628.

Segovia, F., Górriz, J., Ramírez, J., Salas-Gonzalez, D., Álvarez, I., López, M., and Chaves, R. (2012). A comparative study of feature extraction methods for the diagnosis of Alzheimer's disease using the ADNI database. *Neurocomputing*, 75(1):64 – 71.

Varma, S. and Simon, R. (2006). Bias in error estimation when using cross-validation for model selection. *BMC Bioinformatics*, 7(91).

Zhang, D., Wang, Y., Zhou, L., Yuan, H., and Shen, D. (2011). Multimodal classification of Alzheimer's disease and mild cognitive impairment. *NeuroImage*, 55(3):856–867.